

Structure and Stability of a Homologous Series of Tin Oxides

Atsuto Seko,^{1,*} Atsushi Togo,^{2,†} Fumiyasu Oba,² and Isao Tanaka^{2,3}

¹Pioneering Research Unit for Next Generation, Kyoto University, Kyoto 615-8530, Japan

²Department of Materials Science and Engineering, Kyoto University, Kyoto 606-8501, Japan

³Nanostructure Research Laboratory, Japan Fine Ceramics Center, Atsuta, Nagoya, 456-8587 Japan

(Received 25 August 2007; published 30 January 2008)

The structures and stabilities of a series of nonstoichiometric SnO_{2-x} compounds, which are yet unknown experimentally, are predicted using the cluster expansion technique combined with first-principles calculations. A homologous series of $\text{Sn}_{n+1}\text{O}_{2n}$ in which oxygen vacancies are layered on (101) planes of the rutile lattice is discovered. The homologous crystals are composed of divalent and quadrivalent Sn atoms. No trivalent Sn atoms are formed.

DOI: 10.1103/PhysRevLett.100.045702

PACS numbers: 81.30.Dz, 61.50.Ah, 61.66.Fn, 61.72.Bb

The oxides with quadrivalent cations often form a rutile-type structure. Two minerals with this structure known as rutile (TiO_2) and cassiterite (SnO_2) have been popular subjects of fundamental studies for over a century. These oxides are also important in modern technology as catalysts and in spintronic and optoelectronic applications. Both of them often show oxygen deficiency, which plays a central role in determining their properties and chemical activities. In the Ti-O system, a series of nonstoichiometric compounds or homologous compounds are known to exist and are called “Magnéli phase” [1–3]. Many studies have also been carried out on the nonstoichiometric compounds of SnO_{2-x} [4–14]. However, the structures and stabilities are much less understood. Although several phase diagrams have been reported for the Sn-O binary system, they do not agree with each other [4,5]. Even the stability of the monoxide, SnO, has not been well established. Some studies have reported that SnO is a stable phase at a temperature range from 298 K to 543 K [4]. Another group did not show SnO in their equilibrium phase diagram [5]. The structures and stabilities of intermediate compounds, such as Sn_2O_3 , Sn_3O_4 , and Sn_5O_6 , are still open to debate. Recently, possible structures of Sn_2O_3 were discussed theoretically using first-principles calculations through the examination of eight candidate structures [8]. However, their selection of the structures is far from complete and thus is not persuasive. Structures should be searched for within much larger degrees of freedom. For the other nonstoichiometric SnO_{2-x} compounds, no first-principles studies have thus far been reported. To determine the unknown structures, a theoretical approach combining first-principles calculations with a cluster expansion technique [15–17] can be a powerful tool. In the present study, a systematic study of the nonstoichiometric compounds in the Sn-O binary system is carried out by the combined approach.

In general, nonstoichiometry originates from various kinds of point defects. They often form extended structures. To evaluate the thermodynamics of the nonstoichiometric structures, the formation energies of all different defects and their extended structures should be known in

principle. In the practical level, an appropriate modeling of the defective structures is essential for experimentally structure-unknown systems. In the present case of the Sn-O system, no experimental structures have been reported except for SnO and SnO_2 . SnO and SnO_2 have litharge (α -PbO) and rutile structures, as shown in Fig. 1(a). Figure 1(b) illustrates the projections of the structures of SnO and SnO_2 to the (010) plane. They have common features although their space group and the fractional positions of oxygen atoms are different. Tin atoms form a body-centered-tetragonal sublattice in both SnO and SnO_2 . Six oxygen atoms are coordinated to each tin atom in SnO_2 . In SnO, half the oxygen atoms are removed from rutile SnO_2 , as shown in Fig. 1(b). The other oxygen atoms are asymmetrically coordinated to the tin atoms. From the inspection of these structures, we have adopted the oxygen sublattice model for the intermediate structures in which SnO_{2-x} ($0 < x < 1$) is described by the arrangements of oxygen atoms and vacancies on the oxygen sublattice of the rutile SnO_2 . We have also examined the formation energies of a series of nonstoichiometric SnO_{2-x} compounds using the well-known TiO_{2-x} Magnéli structures. The formation energy of the Magnéli structure for Sn_4O_7 is found to be more than +400 meV/cation with reference to SnO (litharge) and SnO_2 (rutile), which is prohibitively high. This implies that the origin of the nonstoichiometry

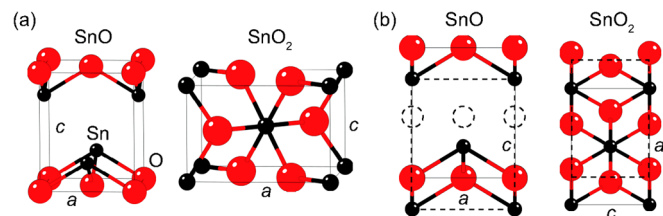


FIG. 1 (color online). (a) Structures of litharge SnO and rutile SnO_2 . Both SnO and SnO_2 show tetragonal symmetry. Experimental lattice constants of SnO and SnO_2 are $a = 3.850 \text{ \AA}$, $c = 4.901 \text{ \AA}$ and $a = 4.738 \text{ \AA}$, $c = 3.188 \text{ \AA}$, respectively. (b) Projections of the structures to (010) plane. The broken circles in SnO correspond to removed oxygen atoms from rutile SnO_2 .

or the multivalency in the Sn-O system is different from that in the Ti-O system although both TiO_2 and SnO_2 have the rutile structure.

After determining the model used to describe the configurational energetics, first-principles total energies of structures in which atoms are arranged in accordance with the model are required to construct the effective Hamiltonian. We need to describe the precise configurational energetics of the pseudobinary oxygen-vacancy system in the oxygen sublattice to investigate the phase stability of the nonstoichiometric structures. It is, however, practically impossible to calculate configurational energies from first principles for all possible structures due to computational costs. A combination of first-principles calculations and a cluster expansion, which provides an effective configurational Hamiltonian in multicomponent systems, enables us to overcome this difficulty. Within the cluster expansion formalism, the configurational energy E can be expressed as

$$E = V_0 + \sum_i V_i \sigma_i + \sum_{i,j} V_{ij} \sigma_i \sigma_j + \sum_{i,j,k} V_{ijk} \sigma_i \sigma_j \sigma_k + \dots, \quad (1)$$

where the coefficients V are called effective cluster interaction (ECI) and σ_i denotes the pseudospin configuration variable for the respective lattice site i ; if the lattice site i is occupied by an oxygen atom (vacancy), then $\sigma_i = 1$ ($\sigma_i = -1$). The values of ECI were determined from the set of first-principles total energies of ordered structures using a least-squares method. The number of structures usually ranges 30–100 to estimate ground states and phase diagrams in close-packed systems. In the Sn-O system, more structures to calculate energies from first principles are indispensable in order to obtain more ECIs than those in the closed-packed systems. This is because the rutile structure has lower symmetry than the close-packed lattice and the effects of lattice relaxations are large as expected from the large difference in the lattice constants between SnO and SnO_2 . We calculated the total energies for 750 ordered structures in which oxygen atoms and vacancies are placed on the oxygen sublattice. These structures include an initial set of random structures and some lower energy structures iteratively refined through the cluster expansion. The computed structures have various numbers of atoms ranging up to 48 atoms. For the calculation of the total energies, we used the projector augmented-wave method [18] within the generalized gradient approximation [19] as implemented in the VASP code [20–22]. Sn-5s, 5p and O-2s, 2p were treated as valence. The plane-wave cutoff energy was set at 300 eV. The total energies were converged to less than 10^{-5} eV. The atomic positions and lattice constants were relaxed until the residual forces became less than 0.01 eV/Å. A set of ECI used to construct the effective Hamiltonian were optimized using a genetic algorithm (GA) [23], which is an evolutionary algorithm used to solve optimization problems. The set of ECI minimizes

the cross-validation score (CV) [24,25], which can determine the accuracy of the cluster expansion that a selected set of ECI reproduces the physical properties well. We eventually selected 28 clusters consisting of the empty and point clusters, 13 pairs, 9 triplets, and 4 quadruplets from 262 clusters up to quadruplets using GA. The corresponding CV was 18.2 meV/anion site. Once the optimal set of ECI is known and the effective Hamiltonian is constructed, one can predict the stable phases and all the configuration-dependent thermodynamical properties on the basis of statistical mechanics. We used the CLUPAN code [26–28] for a series of calculations such as optimization of clusters and the successive searches for stable phases.

There are two kinds of approaches that can be used to find the stable structures using the obtained effective Hamiltonian. One is an exhaustive search by calculating the energies for all possible configurations in a finite-sized cell. This is the most precise way to search for stable structures. However, the space of the search is obviously limited by computational resources. An alternative way is to use some efficient algorithms to solve optimization problems such as simulated annealing (SA) [29,30]. A much larger space of structures can be searched using larger supercells than that by the exhaustive search. Figure 2(a) shows the calculated formation energies relative to the energies of litharge SnO and rutile SnO_2 using the effective Hamiltonian for all configurations within seven different kinds of supercells that are composed of less than 32 oxygen sites. Several structures show singularly low energies. The structure having the lowest energy for Sn_2O_3 ($x = 0.5$) is illustrated in Fig. 2(b). The other low-energy structures have similar features to this structure with oxygen vacancies stacked on the (100) layer. They consist of SnO_2 -like local structures including SnO_6 octahedrons and SnO-like local structures in which Sn atoms face each other. We also performed SA using larger super-

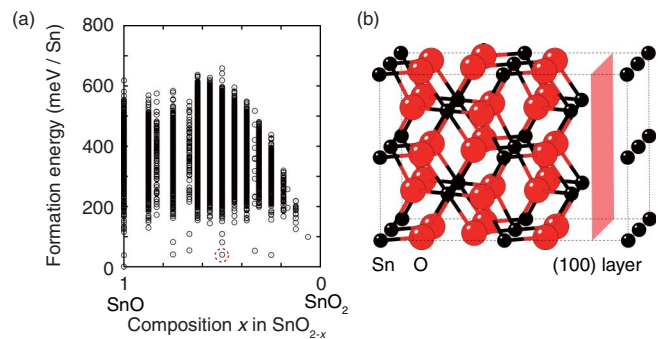


FIG. 2 (color online). (a) Calculated formation energies using the effective Hamiltonian for all structures in which oxygen atoms and vacancies are placed on seven different kinds of supercells that are composed of less than 32 oxygen sites. (b) Structure having the lowest energy for Sn_2O_3 viewed from near the [010] direction. The corresponding energy is shown by the broken circle in (a). Oxygen vacancies forming a (100) layer in the structure are shown by the quadrangle.

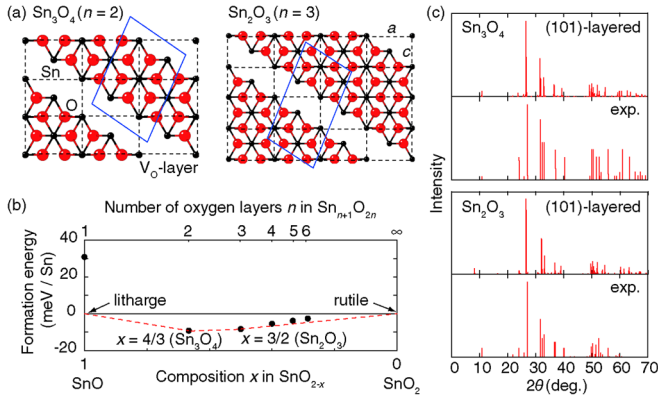


FIG. 3 (color online). (a) Predicted stable structures for Sn_3O_4 and Sn_2O_3 by simulated annealing. The blue solid quadrilaterals show unit cells. (b) Formation energies of (101)-layered structures, shown by closed circles, relative to litharge SnO and rutile SnO_2 . The closed circle at $x = 1$ (SnO) indicates the formation energy of the hypothetical (101)-layered structure for SnO compound. The broken line represents the convex hull of the ground state. (c) Theoretical XRD patterns (Cu-K_α) of the predicted structures for Sn_3O_4 and Sn_2O_3 compared with the experimental XRD patterns reported in Refs. [9,10], respectively.

cells up to $12 \times 12 \times 12$ (10 368 atoms). More stable structures for Sn_3O_4 and Sn_2O_3 are found by SA as shown in Fig. 3(a). The structural parameters and space groups are listed in Table I. In the predicted structures, oxygen vacancies are aligned along the plane corresponding to (101) of SnO_2 . They are composed of SnO_2 -like and SnO -like local structures. Similar structures for the other oxygen-deficient compounds using various sizes of supercells were also predicted by SA. The (101)-layered structures can be expressed as a series of homologous structures of $\text{Sn}_{n+1}\text{O}_{2n}$ with alternating n layers of SnO_2 -like bands and a (101) vacancy layer. Mäki-Jaskari *et al.* calculated the energies for eight possible crystals and interfaces for Sn_2O_3 [8]. Our extensive exploration of the stable structures coincides with their conclusion that the most stable one is the (101)-layered crystal. To discuss the relative stability of $\text{Sn}_{n+1}\text{O}_{2n}$, it is preferable to use first-principles energies because the magnitudes of energy differences among $\text{Sn}_{n+1}\text{O}_{2n}$ with the order of a few millielectron volts per Sn atom are too small to be accurately evaluated using the effective Hamiltonian. Figure 3(b) shows the formation energies of the (101)-layered structures obtained from first principles. Other than $n = 1$, the formation energies are negative. Both Sn_3O_4 ($n = 2$) and Sn_2O_3 ($n = 3$) are

stable, and the other (101)-layered structures ($n = 1, 4-6$) are metastable. However, considering the tiny energy differences among $\text{Sn}_{n+1}\text{O}_{2n}$ ($n = 2-6$), the metastable structures may also be observed by experiments.

Although the structures of SnO_{2-x} compounds have not been determined experimentally, x-ray diffraction (XRD) patterns of two possible compounds have been reported for the compositions of Sn_3O_4 and Sn_2O_3 [9,10]. Figure 3(c) shows the theoretical XRD patterns of the stable structures for Sn_3O_4 and Sn_2O_3 compared with the experimental powder XRD patterns. The theoretical XRD patterns for the predicted (101)-layered structure of Sn_3O_4 and Sn_2O_3 are very close to each other, reflecting the similarities of the structures based on the common SnO and SnO_2 -like units. The peak positions and relative intensities of the theoretical XRD patterns are close to those of the experimental XRD patterns [31]. The agreements of the theoretical and experimental XRD patterns indicate that the Sn_3O_4 and Sn_2O_3 phases observed experimentally in tin oxide systems correspond to the (101)-layered structures based on the mother rutile structure. Recently transmission electron microscope observation of SnO_{2-x} thin film was reported [7]. Nonstoichiometric SnO_{2-x} was found to be formed during annealing a SnO thin film in air before it eventually transformed to the rutile-type SnO_2 . The SnO_{2-x} film showed a number of planer faults that are parallel to the SnO_2 (101) plane. The formation of the faults was ascribed to the presence of oxygen deficiency. Although information of atomic structures was not reported in the Letter, the formation of (101)-type planer faults in the nonstoichiometric composition is consistent with the structure predicted in the present study.

The electronic structures of the homologous phases are investigated together with two reference phases, SnO_2 and SnO . They can be most clearly compared with the projected density of states (PDOS) of Sn atoms. Figure 4 shows the PDOS of two kinds of Sn atoms in Sn_2O_3 along with the PDOS of Sn atoms in SnO_2 and SnO . The Sn(a) atoms, as highlighted in Fig. 4, are coordinated by six oxygen atoms. Therefore, they have a similar local environment as in SnO_2 . The relative positions of the Sn-5s and 5p PDOS and their energies with respect to the Fermi energy are analogous to those of the quadrivalent Sn atom in rutile SnO_2 . The Sn(b) in Fig. 4, on the other hand, is analogous to the divalent Sn atom in SnO . The hybridization of Sn-5s and 5p states can be found at the top of the valence band where O-2p states also exist. The hybridization is related to the formation of the lone pairs,

TABLE I. Predicted structures of the (101)-layered Sn_3O_4 and Sn_2O_3 compounds.

| | Space group | a (Å) | b (Å) | c (Å) | α | β | γ | Atomic fractional coordinates |
|-------------------------|-------------|---------|---------|---------|----------|---------|----------|--|
| Sn_3O_4 | $P2_1/c$ | 8.21 | 4.93 | 5.85 | 90 | 94.7 | 90 | Sn (0.500, 0.000, 0.500), (0.826, 0.000, 0.707) O (0.733, 0.675, 0.503), (0.403, 0.698, 0.774) |
| Sn_2O_3 | $P2_1/c$ | 11.12 | 4.89 | 5.84 | 90 | 77.1 | 90 | Sn (0.370, 0.000, 0.329), (0.122, 0.997, 0.106) O (0.198, 0.699, 0.858), (0.702, 0.677, 0.447), (0.050, 0.307, 0.347) |

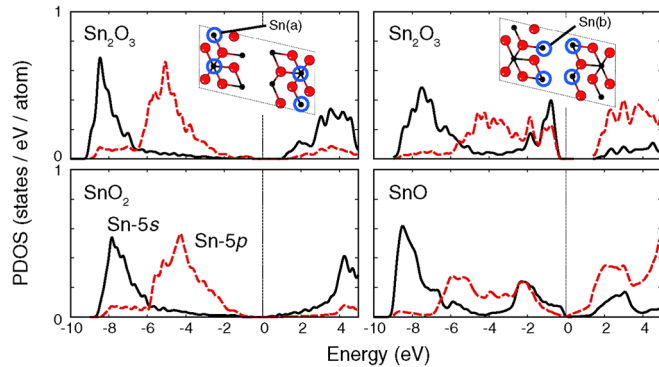


FIG. 4 (color online). PDOS of sixfold-coordinated Sn(a) and asymmetrically oxygen-coordinated Sn(b) in the (101)-layered Sn_2O_3 . The PDOS of Sn atoms in rutile SnO_2 and that of Sn atoms in litharge SnO are shown for comparison.

which is the characteristics of the divalent Sn, as discussed for SnO [32]. These results imply that Sn(a) and Sn(b) in Sn_2O_3 are quadrivalent and divalent, respectively. No other kinds of Sn atoms are present, which indicates the absence of trivalent Sn in Sn_2O_3 . The same conclusion is obtained for Sn_3O_4 and the other layered homologous tin oxides. The nonstoichiometric tin oxides thus show a homologous series of $\text{Sn}_{n+1}\text{O}_{2n}$ in which divalent Sn atoms are facing each other across the oxygen vacancy layer on the (101) plane. The structures of the homologous series of $\text{Sn}_{n+1}\text{O}_{2n}$ should originate from the formation of the lone pairs. Atomic structures and electronic mechanism behind the nonstoichiometric structures are markedly different between two rutile-type oxides of quadrivalent cations, i.e., TiO_2 and SnO_2 .

In this study, we investigated the structures and phase stabilities of rutile-type tin oxides, combining first-principles calculations with the cluster expansion technique, in particular, those of the controversial Sn_2O_3 and Sn_3O_4 intermediate compounds. We predicted a homologous series of $\text{Sn}_{n+1}\text{O}_{2n}$ in which oxygen vacancies are layered on (101) planes. The theoretical structures are consistent with experimental x-ray diffraction profiles. The homologous structures consist of quadrivalent and divalent tin atoms. No trivalent Sn atoms are formed. The present first-principles prediction can trigger atomic-scale experiments such as hyperfine interaction measurements that can verify the extended-defect structures of SnO_{2-x} .

This study was supported by Program for Improvement of Research Environment for Young Researchers from Special Coordination Funds for Promoting Science and Technology (SCF) commissioned by the Ministry of Education, Culture, Sports, Science and Technology (MEXT) of Japan.

*seko@cms.mtl.kyoto-u.ac.jp

- [†]Present address: Institut für Anorganische Chemie, Rheinisch-Westfälische Technische Hochschule Aachen (RWTH), Landoltweg 1, 52056 Aachen, Germany.
- [1] S. Andersson and A. Magnéli, *Naturwissenschaften* **43**, 495 (1956).
 - [2] S. Andersson, B. Collen, U. Kuylenstierna, and A. Magnéli, *Acta Chem. Scand.* **11**, 1641 (1957).
 - [3] J. S. Andersson and B. G. Hyde, *J. Phys. Chem. Solids* **28**, 1393 (1967).
 - [4] G. H. Moh, *Chem. Erde* **33**, 243 (1974).
 - [5] D. J. McPherson and M. Hanson, *Trans. ASME* **45**, 915 (1953).
 - [6] S. Cahen, N. David, J. M. Fiorani, A. Maître, and M. Vilasi, *Thermochim. Acta* **403**, 275 (2003).
 - [7] X. Q. Pan and L. Fu, *J. Appl. Phys.* **89**, 6048 (2001).
 - [8] M. A. Mäki-Jaskari and T. T. Rantala, *Model. Simul. Mater. Sci. Eng.* **12**, 33 (2004).
 - [9] F. Gauzzi, *Ann. Chim. (Paris)* **53**, 1503 (1963).
 - [10] V. G. Murken and M. Trömel, *Z. Anorg. Allg. Chem.* **397**, 117 (1973).
 - [11] H. Giefers, F. Porsch, and G. Wortmann, *Solid State Ionics* **176**, 199 (2005).
 - [12] M. S. Moreno, G. Punte, G. Rigotti, R. C. Mercader, A. D. Weisz, and M. A. Blesa, *Solid State Ionics* **144**, 81 (2001).
 - [13] M. S. Moreno, A. Varela, and L. C. Otero-Díaz, *Phys. Rev. B* **56**, 5186 (1997).
 - [14] Ç. Kılıç and A. Zunger, *Phys. Rev. Lett.* **88**, 095501 (2002).
 - [15] J. M. Sanchez, F. Ducastelle, and D. Gratias, *Physica (Amsterdam)* **128A**, 334 (1984).
 - [16] D. de Fontaine, *Solid State Physics* (Academic Press, New York, 1994), Vol. 47.
 - [17] F. Ducastelle, *Order and Phase Stability in Alloys* (Elsevier Science, New York, 1994).
 - [18] P. E. Blöchl, *Phys. Rev. B* **50**, 17953 (1994).
 - [19] J. P. Perdew, K. Burke, and M. Ernzerhof, *Phys. Rev. Lett.* **77**, 3865 (1996).
 - [20] G. Kresse and J. Hafner, *Phys. Rev. B* **47**, R558 (1993).
 - [21] G. Kresse and J. Furthmüller, *Phys. Rev. B* **54**, 11169 (1996).
 - [22] G. Kresse and D. Joubert, *Phys. Rev. B* **59**, 1758 (1999).
 - [23] G. L. W. Hart, V. Blum, M. J. Walorski, and A. Zunger, *Nat. Mater.* **4**, 391 (2005).
 - [24] M. Stone, *J. R. Stat. Soc. Ser. B Methodol.* **36**, 111 (1974).
 - [25] A. van de Walle and G. Ceder, *J. Phase Equilib.* **23**, 348 (2002).
 - [26] A. Seko, <http://sourceforge.net/projects/clupan> (2007).
 - [27] A. Seko, K. Yuge, F. Oba, A. Kuwabara, I. Tanaka, and T. Yamamoto, *Phys. Rev. B* **73**, 094116 (2006).
 - [28] A. Seko, K. Yuge, F. Oba, A. Kuwabara, and I. Tanaka, *Phys. Rev. B* **73**, 184117 (2006).
 - [29] S. Kirkpatrick, C. D. Gelatt, and M. P. Vecchi, *Science* **220**, 671 (1983).
 - [30] S. Kirkpatrick, *J. Stat. Phys.* **34**, 975 (1984).
 - [31] In both Refs. [9,10], powder samples were obtained by the disproportionation of SnO . In the case of Sn_2O_3 (Ref. [10]), the stoichiometry was determined by the weight gain of the sample during the reaction. Some residual XRD peaks of SnO_2 were subtracted by the authors of Ref. [10].
 - [32] A. Walsh and G. W. Watson, *Phys. Rev. B* **70**, 235114 (2004).